ORIGINAL PAPER

Electrodeposited mixed ZnS–CdS photoelectrode for natural dye-sensitized solar cells (NDSSC)

B B Panda[1]*, P K Mahapatra[2] and M K Ghosh[3]

[1]Department of Chemistry, IGIT Sarang, Dhenkanal, Odisha 759146, India

[2]G. M. College, Sambalpur, Odisha 768004, India

[3]Department of Chemistry, Palsama College, Deogarh, Odisha 768109, India

Abstract: Photoelectrodes and sensitizers are the vital components of future low-cost dye-sensitized solar cells which are used to meet the present energy demand. Herein, ZnS–CdS thin film photoelectrodes (WE) prepared on steel substrate by electrodeposition method are sensitized by chlorophyll extract and combined with graphite counter electrode, both being dipped in sulphide–polysulphide redox electrolytes (S^{2-}/S_n^{2-}) to form the dye-sensitized solar cells with the following configuration:photoelectrode + dye//Na$_2$S(1M) + NaOH(1M) + S(1M)//C(Graphite).The photoelectrochemical characterizations of the dye-sensitized thin film photoelectrodes under investigation include current–voltage (I–V) characteristics in dark and light, spectral photoresponse and cells power output. Photoelectrodes are found to be n-type semiconductors. From the power output curves, the light-to-electricity conversion efficiency of dye-sensitized ZnS–CdS electrode (8 h sensitization)-based solar cells, short-circuit current density (J_{sc}) and open-circuit voltage (V_{oc}) is found to be 0.29, 0.51 mA/cm^2 and 0.34 V respectively. The PXRD results show that the fabricated mixed ZnS–CdS thin films are made up of nanocrystals of size ∼ 9.12 nm. Surface morphology of the films is studied, and SEM micrograms establish the polycrystalline nature of mixed ZnS–CdS thin films. The EDAX (energy diffraction analysis of X-ray) results show the presence of Zn, Cd and S in the thin films.

Keywords: PXRD; SEM image; Chalcogenides; Thin films; Liquid Junction; Mixed compound photoelectrodes

1. Introduction

Rapid urbanization, growth of population and industrial evolution result in an extraordinary increase in global energy demand. Electrical energy which is used extensively by majority of people in the world is primarily produced from fossil fuels such as coals, natural gases and crude oils. These fossil fuels being non-renewable cannot be regenerated in short duration and on burning cause environmental pollution due to emission of greenhouse gases, anthropomorphic climate change, health hazards and global warming. In order to address the dangerous effects of fossil fuels and their depletion, sustainable energy is the only option as it is replenishable, can be used over and over again, available widely free of cost and helps to reduce the adverse effects of non-renewable sources as stated above.

Out of all the renewable energy sources such as solar, wind and hydropower, solar energy has been found to be the most promising candidate for production of electrical energy [1, 2]. Harvesting of solar energy became easier after the development of photovoltaic technology in which sunlight is directly converted into electricity. The technologies are mostly divided into three groups/generations. First, solar cells are manufactured by single-crystalline semiconductor wafer which are costly, second based on inorganic thin film assembly. Quantum dots and dye-sensitized solar cells are the third-generation solar cells which are economical, environmental friendly and high efficient devices [3], and more number of photons can be converted to electrical energy [4, 5]. In DSSC, wide band gap semiconductor electrodes are sensitized by dye molecules which are excited by visible light [6]. The elements of IIB–VIA and VA–VIA group of mixed chalcogenide semiconductors are significant materials for photovoltaic applications [7, 8]. A number of materials have been

*Corresponding author, E-mail: binodgcek@gmail.com

studied as photoanode to obtain high efficient DSSCs [9–13]. Yu and Sero have reported that metal sulphides-based DSSCs can adsorb more dye molecules and reduce the backward moment of electrons to dye molecules [14, 15] where aggregations of metal oxide nanostructures have been reported [16, 17]. Among the metal sulphides, ZnS (E_g-3.5 eV) and CdS (E_g-2.4 eV) thin films have been extensively exploited individually as photoanodes in photovoltaic systems [18–23]. Rafea et al. have studied Zn–CdS thin films as a wide band gap window material in heterojunction solar cells [24]. Natural and artificial dyes have been employed since long to sensitize wide band gap semiconductor materials in solar cells [4, 6, 25–28]. Sensitizers are classified as metal complex sensitizers, metal-free organic sensitizers and natural dye sensitizers. The metal complex sensitizers are highly toxic, non-economical and rare, the metal-free organic sensitizers show low conversion efficiency, and formulation is challenging [29–31], whereas natural dyes are easy to extract, low cost and environmental friendly. But efficiency and stability of natural dye-sensitized solar cells (NDSSC) are low [32]. Hence, the latest research on solar cell is focused on NDSSC (natural dye-sensitized solar cells) [33]. The redox systems play important role in DSSCs for generation of dye molecules and charge transportation [32]. These act as internal charge exporter between the working and counter electrode and constantly restore the species involved during the electrochemical process. These also influence the performance and durability of DSSC by affecting the photoelectrochemical parameters [34]. Mostly, iodide/tri-iodide and sulphide/polysulphide redox systems have been employed in liquid junction solar cells. In iodide/triiodide redox couple, iodine is highly corrosive to metals, which may decline the long-term stability of DSSC. I_2 has high vapour pressure which is not appropriate for device encapsulation. I_3^- and other polyiodides show absorbance in visible range, which may lower the efficiency, react with the injected electrons and amplify the dark current. So iodide/triiodide redox couple is not a proper choice for solar cells. It has been seen that sulphide/polysulphide (S_2/S_n^2) redox electrolytes can prevent chalcogenides from degradation during photoelectrochemical process. Jovanovski et al. [35] and Song et al. [36] reported high efficiency and more stable quantum dots-sensitized solar cells (QDSSC) using aqueous sulphide/polysulphide (S_2/S_n^2) redox electrolytes [35, 36]. Gratzel has also reported stable and efficient photoelectrochemical (PEC) cells using sulphide/polysulphide (S^{2-}/S_n^{2-}) redox system [37]. The thin films of metal and mixed metal chalcogenides can be prepared by different methods such as (a) SILAR [38], (b) chemical bath deposition [39], (c) sol–gel [40], hydrothermal/solvothermal [41, 42], (d) electrochemical anodization [43], (e) electro-spinning [44, 45], (f) spray

pyrolysis [46] and (g) atomic layer deposition [47]. Out of the aforesaid method, the electrodeposition method (ED) has been found to be more suitable as it is simple and economical and gives pure deposited metals [48]. The present piece of research is aimed at fabrication of dye-sensitized solar cells by using electrodeposited ZnS–CdS photoanode as working electrodes (WE), sulphide/poly-sulphide (S^{2-}/S_n^{2-}) redox system, chlorophyll dyes as sensitizer and graphite as counter electrode (CE). The illuminating light source is a 30 mW/cm^2 W-bulb. The schematic diagram with electron flow path of the DSSC is Fig. 1.

2. Experimental details

2.1. Materials

Chemicals such as $CdSO_4$, Na_2S, CH_3COCH_3, $ZnSO_4$, NaOH, S and HCl used in our work are of analytical grade. Double distilled water has been employed as solvent in total experiments.

2.2. Preparations of electrolyte, chlorophyll dyes, electrodes and sensitization

The details of preparation of sulphide/polysulphide redox system and chlorophyll dye extraction are given in our previous paper [1]. Steel substrate (2 cm × 2 cm) and a zinc plate (0.5 cm × 0.5 cm) at a distance of 2 cm are dipped in 50 mL decimolar aqueous solution of $ZnSO_4$ (0.1 M) taken in a 100 mL beaker. Electrodeposition of zinc is carried out by passing a current of 2 mA/cm^2 for 2 h followed by anodization of the metal film using 50 mL
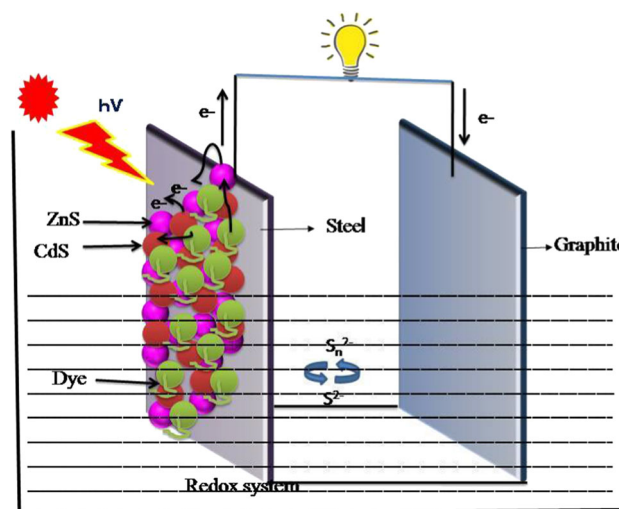

Fig. 1 Schematic diagram with electron flow path of the DSSC

Table 1 Parameters estimated from PXRD of electrodeposited mixed compound (ZnS–CdS) thin film deposited on steel substrate

2θ	θ	(hkl) planes	FWHM	d-spacing	Crystal size (nm)	Dislocation density ($\delta = 1/D^2$)	Strain
22.9369	11.5	100	0.9348	3.87740	9.06	1.2×10^2	2.01×10^{-2}
29.4349	14.7	002	0.9348	3.03455	9.18	1.2×10^2	1.5×10^{-2}

0.1 M Na_2S solution with a current density of 2 mA/cm^2. The same procedure is adopted to deposit CdS on ZnS coated steel substrate by using 0.1 M cadmium sulphate solution. The fabricated electrode is then dipped in 20 mL chlorophyll solution (in acetone) for sensitization. The sensitization is optimized by dipping in the solutions for time periods of 2 h, 4 h, 6 h and 8 h.

2.3. Fabrication of dye-sensitized solar cells

The dye-sensitized solar cells are constructed by combining both ZnS–CdS photoelectrode (WE) and graphite counter electrode (CE) by dipping in the prepared redox electrolyte, and the photoelectrode is illuminated by light intensity of 30 mW/cm^2 intensity. The detailed experimental procedure is given earlier [1].

2.4. Structural, surface morphology and compositional analysis

The powder XRD (X-ray diffraction) is carried out using X-ray diffractometer in the 2θ range of 10°–80° using the step size 0:013 and time step 13.6 s to study the phase, structure and crystallinity of the ZnS–CdS semiconductor. The specification of instrument is given in our earlier report [1]. SEM study is executed by using a Hitachi S-3000 N scanning electron microscope operated at 10 kV, and EDX was carried out on Zeiss EDAX EVO-18 at 15 kV to know the morphology of the crystal of the thin film semiconductor. The crystal size of electrodeposited ZnS–CdS thin film has been estimated by Debye–Scherrer's formula (Eq. 1) [49]:

$$D = \frac{k\lambda}{\beta \cos \theta} \tag{1}$$

where D = crystal size, k = 0.94, λ (X-ray wavelength) = 1.54060 Å, β = full width at half maximum in radians, and θ = Bragg's angle.

Besides this, other physical parameters such as strain, dislocation density and lattice parameters of the nanocrystalline thin film are also estimated by using Eqs. 2, 3 and 4 accounting for the prominent picks and are given in Table 1.

$$E_{str} = \frac{\beta \cot}{4} \tag{2}$$

$$\delta = \frac{1}{D^2} \tag{3}$$

$$\frac{1}{d^2} = \frac{4(l^2 + hl + k^2)}{3a^2} + \frac{l^2}{c^2} \tag{4}$$

where D is size of crystal, δ is dislocation density, E_{str} is strain, h, k, l are Miller indices, a, b and c are lattice parameters, and d is lattice spacing.

2.5. Characterizations

The fabricated DSSCs using ZnS–CdS thin film and sensitized thin films as photoanodes are characterized by measuring the current and voltage in dark and light and power output at light intensity 30 mW/cm^2. The characteristics parameters such as dark and light ideality factor (Eqs. 5 and 6), fill factor (Eq. 7), power conversion efficiency (Eq. 8), shunt resistance (Eq. 9) and series resistance (Eq. 10) have been calculated [1] and are reported in Table 2.

Table 2 Cell characteristic parameters of electrodeposited mixed compound (a) ZnS–CdS and sensitized electrodes, (b) 2 h, (c) 4 h, (d) 6 h and (e) 8 h (Fig. 10)

Substrate	J_{sc} (mA/cm^2)	V_{oc} (V)	FF	Eff (%)	IF dark	IF light	R_s (ohm cm^2)	R_{sh} (ohm cm^2)
ZnS/CdS	0.458	0.311	0.39	0.19	1.2	12	2500	1628
2 h	0.470	0.319	0.37	0.19	1.6	9.4	2000	1147
4 h	0.489	0.332	0.45	0.24	1.6	8.7	2222	1573
6 h	0.498	0.338	0.47	0.26	1.5	7	2500	2058
8 h	0.510	0.340	0.50	0.29	1.6	5.7	2000	2000

$$I = I_0 \left(e^{\frac{eV}{n_d kT}} - 1 \right) \tag{5}$$

$$V_{oc} = \frac{n_1 kT}{q} \ln \frac{I_{sc}}{I_o} \tag{6}$$

$$ff = \frac{I_m \times V_m}{V_{oc} \times I_{sc}} \tag{7}$$

$$\eta = \frac{I_m \times V_m}{P_{input}} \tag{8}$$

$$\left(\frac{\partial I}{\partial V} \right)_{V=0} \cong \frac{1}{R_{sh}} \tag{9}$$

$$\left(\frac{\partial I}{\partial V} \right)_{I=0} \cong \frac{1}{R_s} \tag{10}$$

Here, I_0 = reverse saturation current, e = charge of electron, I = forward bias current, k = Boltzmann constant, V = forward bias voltage, T = temperature, q = charge of electron, V_{oc} = open-circuit voltage, I_{sc} = short-circuit current density, η = energy conversion efficiency, R_s = series resistance, P_{input} = total incident power density, R_{sh} = shunt resistance, n_1 = ideality factor in light and n_d = dark ideality factor.

3. Results and discussion

3.1. X-ray diffraction spectroscopy

The synthesized ZnS–CdS thin film has been characterized using powder X-ray diffraction (PXRD). The PXRD pattern (Fig. 2) shows two strong peaks at 22.9° (100) and 29.4° (002) with a number of small peaks at 31° (101), 35° (102), 44.8° (110), 48.5° (103) and 50.5° (200) planes with
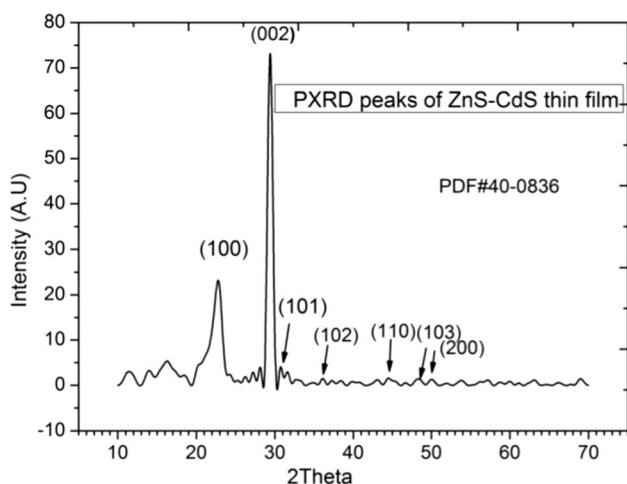

Fig. 2 PXRD pattern of electrodeposited mixed compound (ZnS–CdS) thin film deposited on steel substrate

hexagonal phase of ZnCdS nanoparticles (PDF#40-0836) which is in agreement with the results reported earlier [50, 51]. The crystal size is estimated using relation 1 and found to be 9.12 nm. The lattice parameters are also calculated employing relations 2 and 3 and are reflected in Table 1. The lattice constant estimated using relation 4 is found to be a = 4.5 Å and c = 6.07 Å which is agreed with the results reported by [52]. The formation of more peaks in the PXRD pattern attributes to the polycrystalline nature of ZnS–CdS thin film [51]. Non-appearance of diffraction peaks for CdS (PDF-00-001-0780) and ZnS (PDF-00-001-0677) shows that the film has no any separated phase for these compounds. The pattern also shows the shifting of peak position which may be due to the formation of ZnS–CdS having Zn and Cd in the ratio of 1:1 which is confirmed from EDAX data [53].

3.2. Morphology

Morphological study is performed by using scanning electron microscope in the magnification range of 8500 to 45,000 (Fig. 3). The micrograms establish the formation of nano-polycrystalline ZnS–CdS thin film. The average size of the crystals has been measured and found to be of about 40 nm width and 60 nm length. The higher size of the crystal may be due to agglomeration. The rubbery nanocrystals morphology of the thin film is suitable for effortless movement of electrons than trapping through the nanoparticles. It can be attributed to better photochemical process [54].

3.3. Elemental investigation

EDAX (energy-dispersive analysis of X-ray) spectrum is an important tool for compositional study. The EDAX of ZnS–CdS electrode (Fig. 4) confirms the presence of Zn, Cd and S along with oxygen and carbon. The unwanted peaks for carbon and oxygen are due to the substrate holder and incomplete oxidation or assimilation of CO_2 by film. The atomic ratio (percentage) of the elements illustrates the development of thin film with $Zn_{0.5}Cd_{0.5}S$ composition.

3.4. Thickness measurement

The width of ZnS–CdS thin film was estimated gravimetrically [19] and found to be 89 μm.

3.5. Optical studies

Optical properties of the fabricated ZnS–CdS thin film and sensitized ZnS–CdS thin films by dipping in chlorophyll solution for 6 h have been investigated taking UV–Vis

Fig. 3 SEM micrograms of electrodeposited mixed compound (ZnS–CdS) thin film deposited on steel substrate in the magnification range of (**a**) 8500 (**b**) 33,000 and (**c**) 45,000
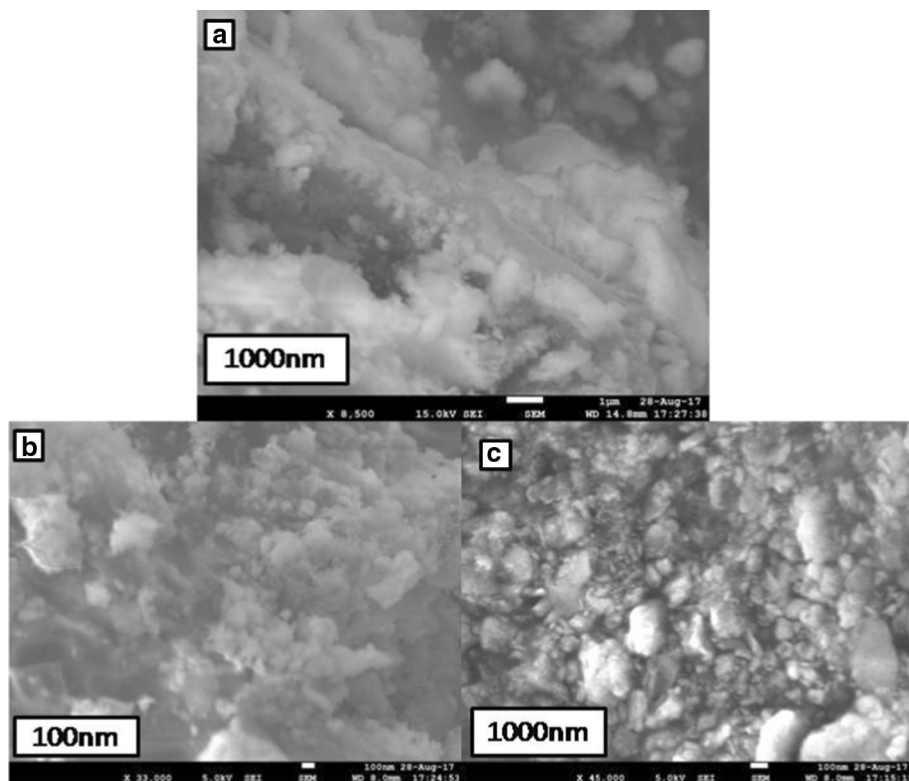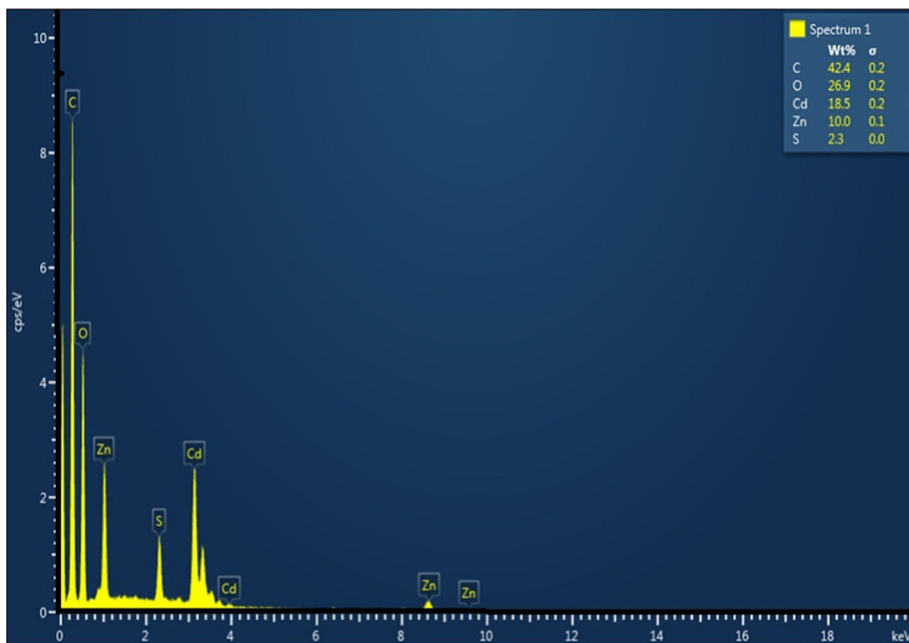

Fig. 4 EDAX spectrum of electrodeposited mixed compound (ZnS–CdS) thin film deposited on steel substrate

absorption spectra in the wavelength range of 200-800 nm (Fig. 5).

The non-appearance of characteristic peaks for chlorophyll [1] in the absorption spectra of dye-loaded ZnS–CdS thin film shows that dye molecules are bonded strongly on the surface of thin films [55]. The band gaps of the ZnS–CdS film have also been calculated using Tauc's Eq. 11 [52]
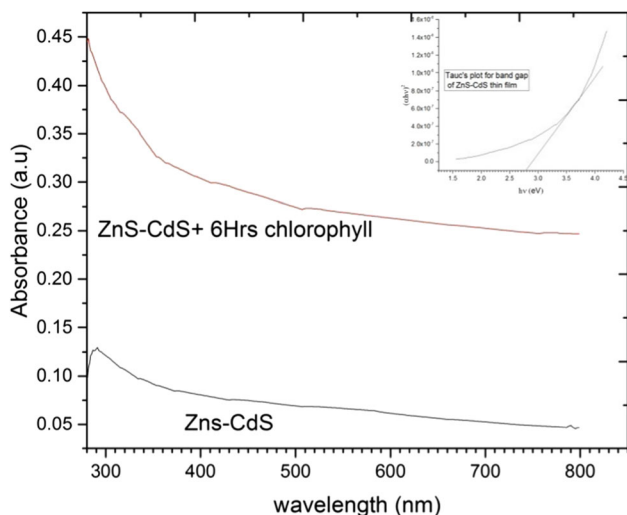
$$\alpha h v = A(h v - E_g)^n \tag{11}$$

Fig. 5 UV–Vis absorption spectra of (**a**) ZnS–CdS thin film, (**b**) 6 h chlorophyll deposited ZnS–CdS thin film and insert of Tauc plot for band gap calculation
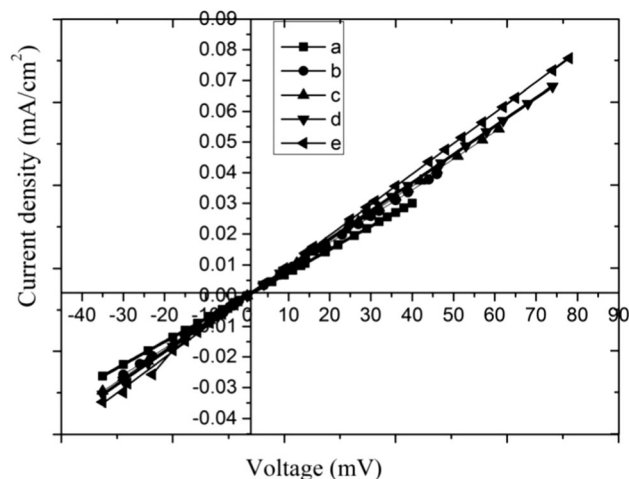

Fig. 7 I–V curves (light) of (**a**) electrodeposited mixed compound (ZnS–CdS) thin film deposited on steel substrate and sensitised films for (**b**) 2 h, (**c**) 4 h, (**d**) 6 h and (**e**) 8 h

Fig. 6 I–V curves (dark) of (**a**) electrodeposited mixed compound (ZnS–CdS) thin film deposited on steel substrate and sensitised films for (**b**) 2 h, (**c**) 4 h, (**d**) 6 h and (**e**) 8 h

Fig. 8 Photoresponse as a function of I_{sc} of (**a**) electrodeposited mixed compound (ZnS–CdS) thin film deposited on steel substrate and sensitised films for (**b**) 2 h, (**c**) 4 h, (**d**) 6 h and (**e**) 8 h

where h = photon energy, A = constant, and $n = 1/2$ for a direct band gap materials.

The optical band gap of the ZnS–CdS has been determined from the plot (insert of Fig. 5) $(\alpha h)^2$ versus h by extrapolating to $(\alpha h)^2 = 0$, and the band gap energy is found to be 2.8 eV.

3.6. Conductivity and I–V characteristics

Figure 6 illustrates the dark current–voltage (I–V) characteristics of the dye-sensitized solar cells using ZnS–CdS and dye-sensitized ZnS–CdS thin films electrodes under
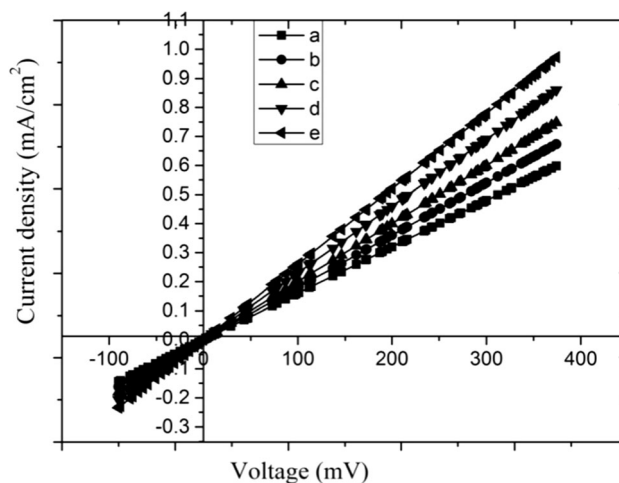
forward and reverse bias at room temperature. The straight lines passing through the origin indicate the formation of ohmic nature films. The non-symmetrical nature signifies the rectifying nature of the fabricated cells with the creation of a p–n junction [56]. Herein, the photodiode might be associated with the innovation of excitons (e$^-$–h$^+$ pairs) by absorbing photon of energy higher than the E_g (band gap) of photoanode, separation and transportation of the e$^-$–h$^+$ pairs by the inter-electric field producing output signal.

The characteristics of photoelectrode–electrolyte interface can be described using current–voltage (I–V) plots in light. The relation of current versus voltage for ZnS–CdS thin film and dye-sensitized thin films is shown in Fig. 7. The shifting of I–V plots toward fourth quadrant under

Fig. 9 Photoresponse as a function of V_{oc} of (a) electrodeposited mixed compound (ZnS–CdS) thin film deposited on steel substrate and sensitised films for (b) 2 h, (c) 4 h, (d) 6 h and (e) 8 h
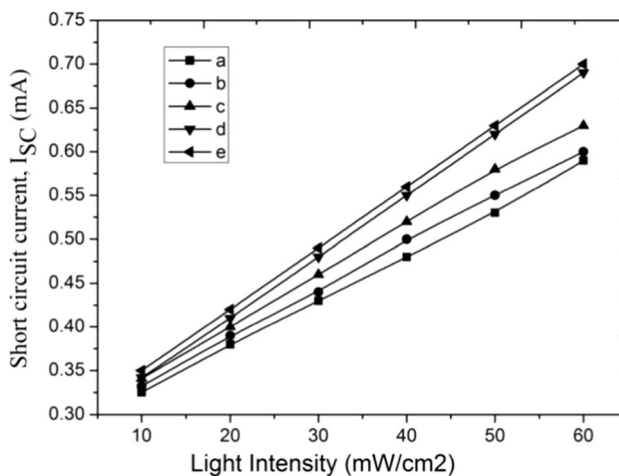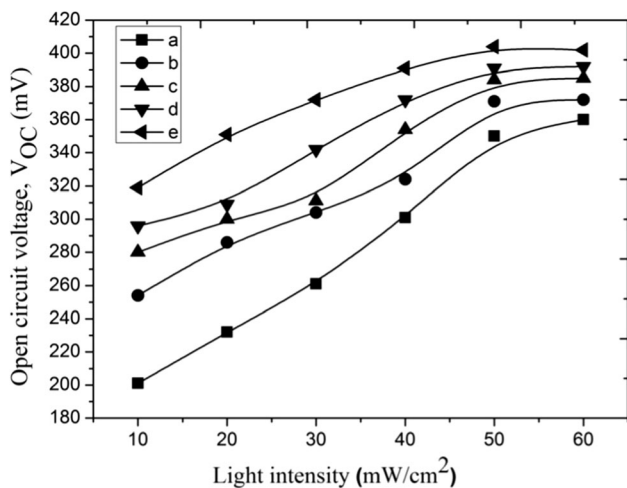

Fig. 11 Log of I_{sc} versus V_{oc} of (a) electrodeposited mixed compound (ZnS–CdS) thin film deposited on steel substrate and sensitised films for (b) 2 h, (c) 4 h, (d) 6 h and (e) 8 h

Fig. 10 Log of I_d versus v in dark of (a) electrodeposited mixed compound (ZnS–CdS) thin film deposited on steel substrate and sensitised films for (b) 2 h, (c) 4 h, (d) 6 h and (e) 8 h
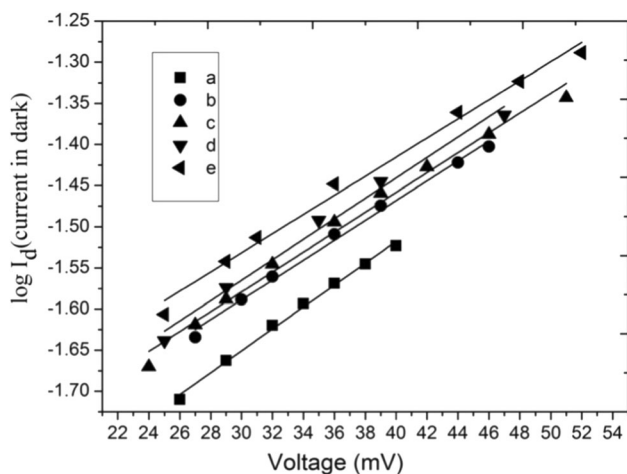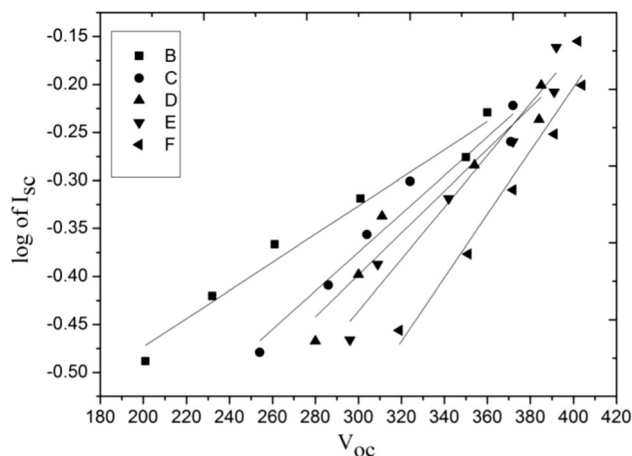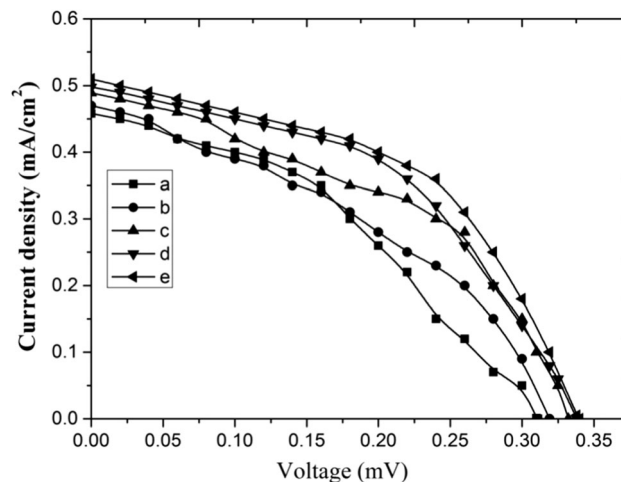

Fig. 12 Power output characteristics curve of (a) electrodeposited mixed compound (ZnS–CdS) thin film deposited on steel substrate and sensitised films for (b) 2 h, (c) 4 h, (d) 6 h and (e) 8 h

illumination attributes the possibility of conversion of photon to electricity by fabricated cell [57]. The absorbed light energy improves the free electron concentration in conduction band and free hole in valence band by breaking covalent bonds [58].

3.7. Photoresponse study

The photoresponses of fabricated cells using ZnS–CdS electrode and dye-sensitized ZnS–CdS electrodes have been studied by measuring the change of I_{sc} versus light intensity and V_{oc} versus light intensity. The change of I_{sc} versus light intensity (Fig. 8) is straight line which

indicates that all photoelectrode–(S^{2-}/S_n^{2-}) electrolyte interfaces can be modelled as Schottky barrier solar cell [59].

Change of V_{oc} versus light intensity (Fig. 9) illustrates the saturation of open-circuit voltage (V_{oc}) which reveals that the interface is saturated, and electrons and holes are dispersed unequally within the space charge area of the semiconductor [18].

3.8. Study of ideality of solar cell

The ideality factor speaks about the extent of agreement of a diode to the ideal diode equation [60]. Higher ideality factor points out the expansion of defects in the crystal which is the reason of abnormal recombination mechanisms [61]. Series resistance and the carrier recombination

within interface also enhance the ideality factor [62]. Heterogeneous thickness of films and multiformity of interfacial charges might be a cause of higher ideality factor [63]. Herein, the dark and light ideality factors are estimated from Figs. 10 and 11 using Eqs. 5 and 6 and reported in Table 2. Data demonstrate that ideality factor (dark) for ZnS–CdS is 1.2, whereas it is 1.6 for sensitized thin films, but the light ideality factors decrease from 12 to 5.7 with the increase in deposition time of chlorophyll.

3.9. Power output study

Figure 12 illustrates the power conversion characteristics of fabricated solar cells using ZnS–CdS thin film and chlorophyll dye-sensitized thin film as photoanode (WE), graphite as cathode (CE) and S^{2-}/S_n^{2-} as redox system under light illumination of 30 mW/cm^2 (area of illumination 1.5 cm^2). The characteristic parameters estimated using the relation (7 and 8) are presented in Table 2. Results illustrate that J_{sc}, V_{oc} and efficiency are continuously increasing from 0.458 mA, 0.311 V and 0.19 to 0.510, 0.340 and 0.29, respectively, with the raise of time for chlorophyll deposition. An increase in J_{sc} and V_{oc} may be reason of the increase in electron density, transportation and lifetime [64]. Results illustrate that power conversion efficiency of fabricated DSSC using 8-h sensitized electrode is 0.29%.

The photoelectrochemical parameters for CdZnS electrode prepared by dip coating as reported by Dongre and group [53] are very low as compared to our results. This illustrates that electrodeposition method is better than dip-coating process. A number of results have also been published on chlorophyll dye sensitization where chlorophyll has been extracted from different sources using different solvents [5, 65–67]. Cerda and co-workers have reported highest efficiency of 0 .04% using black myrtle with V_{oc} of 0.4 V and J_{sc} of 0.02 mA. Syafinar and co-workers have reported J_{sc} of 0.35 mA and V_{oc} of 0.44 V [26]. Our results are higher than those which prove that the transports of electron and density of electron along with lifetime are increasing. Fill factor is another parameter for solar cell characterization which is associated with the highest power generation (P_{max}) of solar cell. In DSSCs, it is found to be low due to parasitic resistance (R_s, R_{sh}) and charge recombination at interface. Higher fill factor can be imagined in DSSC when R_s is low and R_{sh} is high [1].

In our study, fill factor enhances from 0.39 to 0.5 with increase in chlorophyll deposition time which is greater than other workers [5, 65–67]. The R_{sh} and R_s have also been measured using relations 9 and 10 for ZnS–CdS thin film and sensitized thin films and are reported in Table 2. The higher R_s may be due to slow movement of electrons in photoelectrode, low diffusion of ions in the redox system

and resistance of metal in contacts. Similarly, higher R_{sh} may be due to crystal defects. However, the R_{sh} in our study is increasing which may be the cause of the increase in ff, efficiency and decrease in light ideality factors. The decrease in R_{sh} at 8 h deposited sensitized film attributes the increase in crystal defect, and further deposition of chlorophyll may enhance the defect in the crystals.

4. Conclusion

Rubbery nanocrystalline ZnS–CdS thin films have been fabricated by electrodeposition technique and have been sensitized by chlorophyll extracted from the plant Tagetes Patula. The PXRD data prove that the thin film of ZnS–CdS photoelectrode formed is made of hexagonal crystals of size ≈ 9.12 nm. SEM micrograms illustrate that the crystals are agglomerated and EDX spectroscopy confirms the presence of Zn, Cd and S having empirical formula $Zn_{0.5}Cd_{0.5}S$. End result illustrates that wide band gap sulphide materials might be exploited in fabrication of dye-sensitized solar cells employing chlorophyll as sensitizer.

References

[1] B B Panda, P K Mahapatra and M K Ghosh *J. Electron. Mater.* **47** 3657 (2018)

[2] P Zhang, B Y Guan, L Yu and X W David Lou *Chem* **4** 162 (2018)

[3] H K Jun, M A Careem and A K Arof *Renew. Sustain. Energy Rev.* **22** 148 (2013)

[4] H C Hassan, Z H Z Abidin, F I C howdhury and A K Arof *Int. J. Photoenergy* https://doi.org/10.1155/2016/3685210

[5] Y Duan, N Fu, Q Liu, Y Fang, X Zhou, J Zhang and Y Lin *J. Phys. Chem. C* **116** 8888 (2012)

[6] G Calogero, G Di Marco, S Caramori, S Cazzanti, R Argazzic and C A Bignozzi *Energy Environ. Sci.* **2** 1162 (2009)

[7] C S Ferekides, U Balasubramanian, R Mamazza, V Viswanathan, H Zhao and D L Morel *Sol. Energy* **77** 823 (2004)

[8] D J Desale, S Shaikh, A Ghosh, R Birajadar, F Siddiqui, A Ghule and R B Sharma *Compos. B Eng.* **43** 1095 (2012)

[9] M K Nazeeruddin, F De Angelis, S Fantacci, A Selloni, G Viscardi, P Liska, S Ito, B Takeru and M Gratzel *J. Am. Chem. Soc.* **127** 16835 (2005)

[10] R A Jensen, H V Ryswyk, C X She, J M Szarko, L X Chen and J T Hupp *Langmuir* **26** 1401 (2010)

[11] H J Snaith and C Ducati *Nano Lett.* **10** 1259 (2010)

[12] K Hara, T Horiguchi, T Kinoshita, K Sayama, H Sugihara and H Arakawa *Sol. Energy Mater. Sol. Cells* **64** 115 (2000)

[13] S M Yang, H Z Kou, H J Wang, K Cheng and J C Wang *J. Phys. Chem. C* **114** 815 (2010)

[14] X L Yu, J G Song, Y S Fu, Y Xie, X Song, J Sun and X W Du *J. Phys. Chem. C* **114** 2380 (2010)

[15] I M Sero, S Gimenez, F F Santiago, R Gomez, Q Shen, T Toyoda and J Bisquert *Acc. Chem. Res.* **42** 1848 (2009)

[16] Q F Zhang, T R Chou, B Russo, S A Jenekhe and G Z Cao *Angew. Chem. Int. Ed.* **47** 2402 (2008)

[17] Q F Zhang, C S Dandeneau, K Park, D W Liu, X Y Zhou, Y H Jeong and G Z Cao *J. Nanophotonics* **4** 041540 (2010)

[18] P P Hankare, P.A. Chate and D.J. Sathe *J. Alloys Compd.* **487** 367 (2009)

[19] A B Bhalerao, C D Lokhande and B G Wagh *IEEE Trans. Nanotechnol.* **12** (2013)

[20] S Sfaelou, L Sygellou, V Dracopoulos, A Travlos and P Lianos *J. Phys. Chem. C* **118** 22873 (2014)

[21] E Rabinovich and G Hodes *J. Phys. Chem. C* **117** 1611 (2013)

[22] S B Patil and A K Singh *Appl. Surf. Sci.* **256** 2884 (2010)

[23] S A Pawar, D S Patil, A C Lokhande, M G Gang, J C Shin, P S Patil and J H Kim *Opt. Mater.* **58** 46 (2016)

[24] M A Rafea, A A M Farag, N Roushdy *J. Alloys Compd.* **485** 660 (2009)

[25] A Jana, C Bhattacharya and J Datta *Electrochim. Acta* **55** 6553 (2010)

[26] R Syafinar, N Gomesh, M Irwanto, M Fareq and Y M Irwan *Energy Procedia* **79** 896 (2015)

[27] L L Li and E W G Diau *Chem. Soc. Rev.* **42** 291 (2013)

[28] X YaoMing, W JiHuai, C CunXi, C Yuan, Y GenTian, L JianMing, H MiaoLiang, F LeQing and L Zhang *Chin. Sci. Bull.* **57**, 2329 (2012)

[29] P K Mahapatra and B B Panda *Chalcogenide Lett.* **7** 477 (2010)

[30] N Sekar and V Y Gehlot *Resonance* **819** (2010)

[31] G Calogero, J H Yum, A Sinopoli, G D Marco, M Gratzel and M K Nazeeruddin *Sol. Energy* **86** 1563 (2012)

[32] G Richhariya, A Kumar, P Tekasakul and B Gupta *Renew. Sustain. Energy Rev.* **69**, 705 (2017)

[33] M Gratzel *J. Phys. Chem.* **97** 6272 (1993)

[34] L Goncalves, V Bermudez, H Ribeiroa and A Mendes *Energy Environ. Sci.* **1** 655 (2008)

[35] V Jovanovski, V González-Pedro, S Giménez, E Azaceta, G Cabañero, H Grande, R Tena-Zaera, I Mora-Seró and J Bisquer *J. Am. Chem. Soc.* **133**, 20156 (2011)

[36] H Song, H Rao and X Zhong *J. Mater. Chem. A* **6**, 4895 (2018)

[37] M Gratzel *Acc. Chem. Res.* **42** 1788 (2009)

[38] V Chakrapani, D Baker and P V Kamat *J. Am. Chem. Soc.* **133** 9607 (2011)

[39] S Mahajan, E Stathatos, N Huse, R Birajdar, A Kalarakis and R Sharma *Mater. Lett.* **210** 92 (2018)

[40] A S Dive, N P Huse, K P Gattu, R B Birajdar, D R Upadhyay and R Sharma *J. Mater. Sci. Mater. Electron.* https://doi.org/10.1007/s10854-017-7393-5

[41] A Bahramian *Ind. Eng. Chem. Res.* **52** 14837 (2013)

[42] H P Wu, C M Lan, J Y Hu, W K Huang, J W Shiu, Z J Lan, C M Tsai, C H Su and E W G. Diau *J. Phys. Chem. Lett.* **4** 1570 (2013)

[43] Z Q Bao, H Xie, Q Zhu, J Qian, P Ruana and X Zhou *CrystEngComm* **15** 8972 (2013)

[44] N Mir, K Lee, I Paramasivam and P Schmuki *Chem. Eur. J.* **18** 11862 (2012)

[45] H Y Chen, T L Zhang, J Fan, D B Kuang and C Y Su *ACS Appl. Mater. Interfaces* **5** 9205 (2013)

[46] E N Kumar, R Jose, P S Archana, C Vijila, M M Yusoff and S Ramakrishna *Energy Environ. Sci.* **5** 5401 (2012)

[47] J Huo, Y Hu, H Jiang, W Huang, Y Li, W Shao and C Li *Ind. Eng. Chem. Res.* **52** 11029 (2013)

[48] A E Alam, W M Cranton, M Dharmadasa *J. Mater. Sci. Mater. Electron.* **30** 4580 (2019)

[49] H J Son, C Prasittichai, J E Mondloch, L Luo, J Wu, D W Kim, O K Farha and J T Hupp *J. Am. Chem. Soc.* **135** 11529 (2013)

[50] B B Panda, B Sharma and R K Rana *Mater. Sci. Pol.* **34** 446 (2016).

[51] C Duan, W Luo, T Jiu, J Li, Y Wang and F Lu *J. Colloid Interface Sci.* https://doi.org/10.1016/j.jcis.2017.09.108

[52] M A Mahdi, J J Hassan, Z Hassan, S S Ng *J. Alloys Compd.* **541** 227 (2012)

[53] J K Dongre, M Chaturvedi, Y Patil, S Sharma, and U K Jain *AIP Conf. Proc.* **1670**, 030007 (2015). https://doi.org/10.1063/1.4926691

[54] J Song, S S Li, S Yoon, W K Kim, J Kim, J Chen, V Craciun, T J Anderson, O D Crisalle and F Ren 0-7803-8707-4/05/ $20.0002005 IEEE

[55] T Suyitno, T J Saputra, A Supriyanto, Z Arifin *Spectrochim. Acta A Mol. Biomol. Spectrosc.* **148** 99 (2015)

[56] P K Mahapatra and B B Panda *Int. J. Thin Films Sci. Technol.* **4** 45 (2015)

[57] R M Mane, S S Mali, V B Ghanwat, V V Kondalkar, K V Khot, S R Mane, D B Shinde, P S Patil and P N Bhosale *Mater. Today Proc.* **2** 1458 (2015)

[58] A A Yadav and E U Masumdar *J. Alloys Compd.* **509** 5394 (2011)

[59] N P Husea, A S Divea, K P Gattub and R Sharma *Mater. Sci. Semicond. Process.* **67** 62 (2017)

[60] K Rajeshwar, L Thomson, P Singh, R C Kainthala and K L Chopra *J. Electrochem. Soc.* **128** 1744 (1981)

[61] K Alfaramawi *Dig. J. Nanomater. Biostruct.* **5** 933 (2010)

[62] A D A Buba, E O Ajala and D O Samson *Asian J Sci Technol* **6** 1146 (2015)

[63] S M Pawar, A V Moholkar, K Y Rajpure, C H Bhosale *Sol. Energy Mater. Sol. Cells* **92** 45 (2008)

[64] S Aydogan and O Gullu *Microelectron. Eng.* **87** 187(2010)

[65] B Cerda, R Sivakumar, M Paulraj *J. Phys. Conf. Ser.* **720** 012030 (2016) https://doi.org/10.1088/1742-6596/720/1/012030

[66] H Chang, H M Wu, T L Chen, K D Huang, C S Jwo and Y J Lo *J. Alloys Compd.* **495** 606 (2010)

[67] H Chang, M J Kao, T L Chen, C H Chen, K C Cho and X R Lai *Int. J. Photoenergy* 2013; Article ID 159502